

Redistribution of Boron and Fluorine Atoms in BF_2 Implanted Silicon Wafers during Rapid Thermal Annealing

Woo Sik YOO, Takashi FUKADA, Tsuyoshi SETOKUBO¹, Kazuo AIZAWA¹ and Toshinori OHSAWA²

WaferMasters, Inc., 246 East Gish Road, San Jose, CA 95112, U.S.A.

¹NEC Hiroshima Limited, 7-10 Yoshikawa Kogyodanchi, Higashi Hiroshima, Hiroshima 739-0198, Japan

²Tokyo Electron Ltd., 3-6 Akasaka 5-chome, Minato-ku, Tokyo 107-8481, Japan

(Received July 1, 2002; accepted for publication November 14, 2002)

Rapid thermal annealing (RTA) of $^{49}\text{BF}_2^+$ (70 keV , $1 \times 10^{15}\text{ cm}^{-2}$) implanted Si wafers (200 mm in diameter) was carried out using a single wafer furnace-type system and a lamp-based system. Sheet resistance and the uniformity of implanted wafers were measured after annealing under various annealing conditions. Boron and fluorine depth profiles were investigated using secondary ion mass spectroscopy (SIMS) after annealing. Boron atoms diffuse into bulk crystal as annealing progresses, while fluorine atoms move towards the surface and form two peculiar peaks around 65 nm and 105 nm from the surface, regardless of annealing conditions. A significant increase in sheet resistance due to boron clustering near the F peaks was observed in wafers annealed at 1100°C using a lamp-based system. The effects of annealing method, temperature and time on dopant redistribution were discussed. [DOI: 10.1143/JJAP.42.1123]

KEYWORDS: single wafer rapid thermal furnace (SRTF), rapid thermal annealing (RTA), implant anneal, sheet resistance, electrical activation, secondary ion mass spectroscopy (SIMS), dopant redistribution, boron clustering

1. Introduction

Boron difluoride ions ($^{49}\text{BF}_2^+$) are one of the favored ion species often used for shallow and ultra-shallow junction formation due to their amorphization ability and small projected range compared to boron ($^{11}\text{B}^+$) ions at a given implant energy.^{1,2)} $^{49}\text{BF}_2^+$ and $^{11}\text{B}^+$ implanted silicon wafers with the equivalent B depth profile give different sheet resistances and junction depths after rapid thermal annealing (RTA) due to the differences in electrical activation and diffusion characteristics of the B atoms. Secondary ion mass spectroscopy (SIMS) depth profiling of B atoms revealed that $^{49}\text{BF}_2^+$ implanted wafers give shallower junctions than $^{11}\text{B}^+$ implanted wafers. The existence of fluorine is believed to be effective in suppressing boron transient enhanced diffusion (TED).^{3,4)} However, no clear explanation of F redistribution behavior or the role of F in $^{49}\text{BF}_2^+$ implanted Si wafers is available.

To precisely control the junction depth, as well as the sheet resistance of $^{49}\text{BF}_2^+$ implanted Si wafers after annealing, one must understand B and F redistribution behavior and the role of F in $^{49}\text{BF}_2^+$ implanted Si wafers during annealing. In a previous comparative study on implant annealing using a lamp-based rapid thermal annealing (RTP) system and a single wafer furnace-type system, the authors observed the fluctuation of B concentration in some $^{49}\text{BF}_2^+$ implanted wafers after annealing in the lamp-based RTP system, while no fluctuation was observed in wafers annealed using the furnace-type system.⁵⁾ In this work, $^{49}\text{BF}_2^+$ (70 keV , $1 \times 10^{15}\text{ cm}^{-2}$) implanted Si wafers (200 mm in diameter) were annealed under various conditions using the single wafer furnace-type system and lamp-based system. B and F depth profiles were measured to investigate in detail the influence of heating method on electrical activation and dopant (B and F) redistribution. The effects of annealing method, temperature and time on the electrical activation and dopant redistribution characteristics are discussed based on SIMS depth profiles and the wafer heating mechanism.

2. Experimental

$^{49}\text{BF}_2^+$ ions were implanted into 200-mm-diameter n-type Si (100) wafers ($2.0\text{--}8.0\ \Omega\text{-cm}$) with $1.0\text{--}1.5\text{-nm}$ -thick native oxide. Implantation energy and dose levels were 70 keV and $1 \times 10^{15}\text{ cm}^{-2}$, respectively. The implanted wafers were divided into two groups to perform split annealing experiments in both the conventional lamp-based RTP system and the single wafer rapid thermal furnace (SRTF) system. Both systems have been well maintained in a production environment and they were calibrated prior to the experiment. Annealing was carried out under an ambient N_2 atmospheric pressure and the annealing temperature was varied from 900°C to 1100°C . The annealing time was varied between 10 s and 150 s for the lamp-based RTP system. The annealing time for the SRTF system was varied from 40 s to 180 s. The annealing time recorded for the lamp-based RTP system is the soak time near the process temperature regardless of overhead times such as preheating, ramp-up and ramp-down times. The preheating and ramp-up steps usually last for 20–30 s depending on the annealing temperature. If the annealing time (soak time) at the maximum temperature (or plateau) is substantially longer than 1 s, it is generally referred as a “soak anneal”. The annealing time referred to in the SRTF system is the wafer residence time (from wafer-in to wafer-out) in the heated furnace (process chamber) and is equivalent to the ramp-up time plus soak time in the lamp-based RTP system. Thus, the annealing time (residence time) for the SRTF system was determined by simply adding 30 s to the annealing time (soak time) used in the lamp-based RTP system to approximate the thermal history of wafers processed in the lamp-based RTP system. Details of the SRTF system configurations and thermal characteristics, including wafer temperature ramp-up and ramp-down characteristics, are reported in previous publications.^{6–8)}

The sheet resistance (ρ_s) and sheet resistance uniformity of $^{49}\text{BF}_2^+$ implanted wafers were measured using a four-point probe after annealing under various conditions using both the SRTF system and the lamp-based RTP system. For

the sheet resistance measurement, 49 points were measured excluding within 5 mm of the edge of the wafer. B and F depth profiles of the implanted wafers were investigated using SIMS after annealing under the various annealing conditions.

3. Results and Discussion

The average sheet resistances of $^{49}\text{BF}_2^+$ (70 keV $1 \times 10^{15} \text{ cm}^{-2}$) implanted wafers after annealing using the lamp-based RTP system and SRTF system are shown in Figs. 1(a) and 1(b) as a function of annealing temperature and time. As seen in the figure, the behavior of the sheet resistance of $^{49}\text{BF}_2^+$ implanted wafers after annealing is very complex. The results are also dependant on the type of annealing system.

In the wafers annealed using the lamp-based RTP system, the sheet resistance monotonically decreases from 126.6 $\Omega/\text{sq.}$ (for 10 s) to 109.7 $\Omega/\text{sq.}$ (for 150 s) at 900°C due to the progress in electrical activation as the annealing time was increased. The sheet resistance uniformity was improved from 2.3% (1σ) to 0.8% (1σ) as annealing time was increased from 10 s to 150 s. When the annealing was carried out at 1000°C, the sheet resistance monotonically increased from 99.7 $\Omega/\text{sq.}$ to 111.9 $\Omega/\text{sq.}$ as the annealing time was increased from 10 s to 150 s. The sheet resistance uniformities of wafers annealed at 1000°C were all below 0.5% in 1σ . At 1100°C, the sheet resistance increased very rapidly from 109.8 $\Omega/\text{sq.}$ to 215.9 $\Omega/\text{sq.}$ as the annealing time was increased from 10 s to 150 s. The sheet resistance uniformity

deteriorated significantly from 1.4% (1σ) to 10.2% (1σ) as the annealing time was increased from 10 s to 40 s at 1100°C. The sheet resistance uniformity of wafers annealed for 70–150 s at 1100°C was 2.4–3.2% (1σ). The minimum sheet resistance of 99.7 $\Omega/\text{sq.}$ with a sheet resistance uniformity of 0.4% (1σ) was achieved with 10 s annealing at 1000°C.

In the wafers annealed at 900°C and 1000°C using the SRTF system, similar trends in the sheet resistance and sheet resistance uniformity as a function of annealing temperature and time were observed. The wafers annealed at 1100°C also showed a gradual sheet resistance increase with increased annealing time. In wafers annealed at 900°C, the sheet resistance monotonically decreased from 134.3 $\Omega/\text{sq.}$ to 111.3 $\Omega/\text{sq.}$ for 40 s to 180 s due to the progress in electrical activation as the annealing time was increased. The sheet resistance uniformity ranged from 0.3% (1σ) to 0.7% (1σ). At 1000°C, the sheet resistance gradually increased from 100.6 to 109.6 $\Omega/\text{sq.}$ as the annealing time was increased from 40 s to 180 s. The sheet resistance uniformities of wafers annealed at 1000°C were all below 0.5% in 1σ . At 1100°C, the sheet resistance increased at a similar rate, from 104.3 $\Omega/\text{sq.}$ to 116.0 $\Omega/\text{sq.}$, as the annealing time was increased from 40 s to 180 s. The sheet resistance uniformity deteriorated significantly from 0.5% (1σ) to 11.7% (1σ) as the annealing time was increased from 40 s to 180 s. The minimum sheet resistance of 100.6 $\Omega/\text{sq.}$ with a sheet resistance uniformity of 0.2% (1σ) was achieved by annealing at 1000°C for 40 s.

In our previous study, we compared the sheet resistances of three annealed wafers which showed almost identical B depth profiles.⁵⁾ Two wafers were annealed using the lamp-based RTP system. One was annealed at 1100°C for 10 s and the other was annealed at 1000°C for 70 s. The third wafer was annealed at 1000°C for 100 s using the SRTF system. Among them, the wafer annealed at 1100°C for 10 s in the lamp-based RTP system showed the highest sheet resistance value of 109.8 $\Omega/\text{sq.}$ Implant annealing must be performed at an optimum (not necessarily higher) temperature for a reasonable amount of time to achieve the maximum electrical activation with minimum dopant diffusion. The result is contradictory to the basic concept of “spike annealing” proposed by Jennings *et al.*⁹⁾ At a given annealing temperature, the dopant depth profiles are almost identical regardless of the annealing method (or equipment) used, as long as the sheet resistance values are equivalent. Both the high temperature annealing and the long time annealing enhance dopant diffusion. We also found, as a general trend, that a longer annealing around 1000°C gives lower sheet resistance and better sheet resistance uniformity than a short time annealing at 1100°C, regardless of the annealing system. The result poses a question regarding the effectiveness of the “spike annealing”. A “soak annealing” at slightly lower temperatures is proposed as an alternative implant annealing technique for shallow junction formation.⁵⁾ The oscillation of boron concentration was previously observed in $^{49}\text{BF}_2^+$ implanted wafers annealed at 1100°C for more than 25 s in lamp-based RTP systems.

Figure 2 shows the annealing time dependence of sheet resistance values and B depth profiles of $^{49}\text{BF}_2^+$ (70 keV $1 \times 10^{15} \text{ cm}^{-2}$) implanted wafers annealed at 1100°C. The

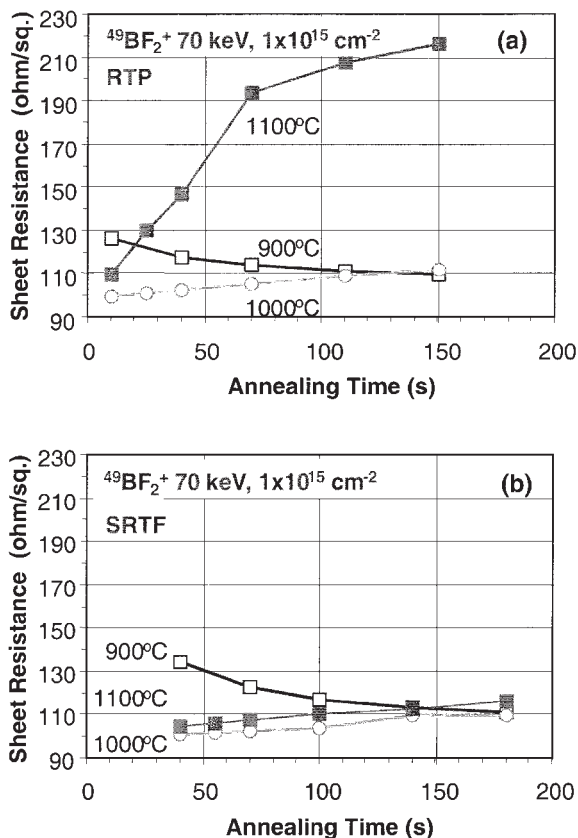


Fig. 1. Sheet resistance of $^{49}\text{BF}_2^+$ (70 keV $1 \times 10^{15} \text{ cm}^{-2}$) implanted wafers as a function of annealing temperature and time. ((a) lamp-based RTP system and (b) SRTF system).

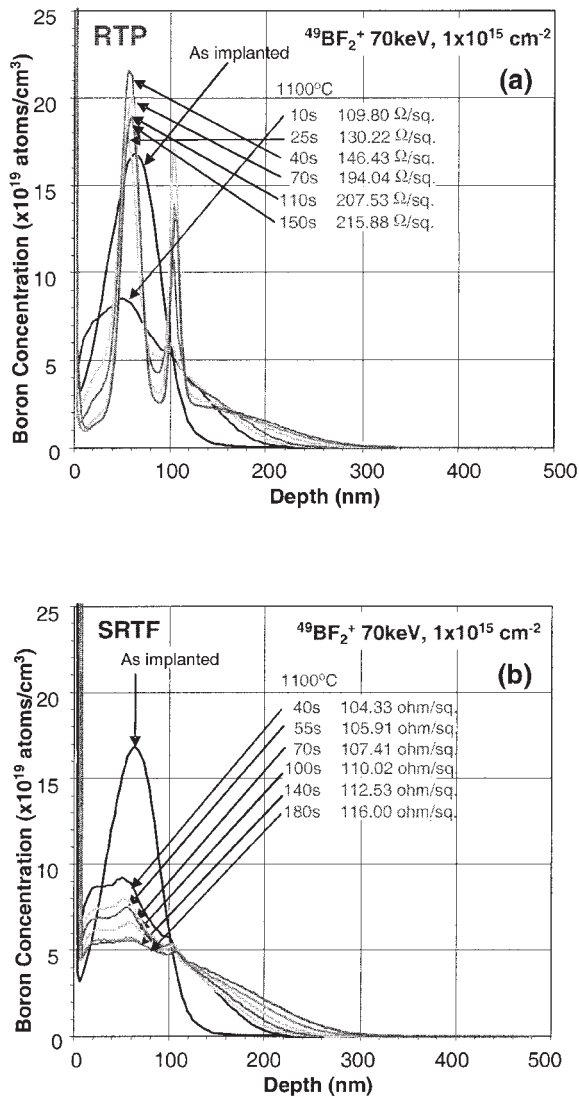


Fig. 2. Annealing time dependence of sheet resistance values and B depth profiles of $^{49}\text{BF}_2^+$ ($70 \text{ keV } 1 \times 10^{15} \text{ cm}^{-2}$) implanted wafers annealed at 1100°C [(a) lamp-based RTP system and (b) SRTF system].

wafers annealed for more than 25 s using a lamp-based RTP system showed B segregation at 65 nm and 105 nm from the surface. The wafer annealed at 1100°C for 10 s showed significant B dopant diffusion. The maximum B concentration around 70 nm from the surface was reduced by a factor of 2.5. When annealing was carried out at 1100°C for more than 25 s, B atoms segregated at the two specific depths of $\sim 65 \text{ nm}$ and $\sim 105 \text{ nm}$. The maximum B concentration (at $\sim 65 \text{ nm}$) of wafers annealed for between 25 s and 150 s exceeded the implanted maximum B concentration. In a 40 s annealed wafer, the B concentration at the two peaks reached maximum. As annealing time is increased from 40 s, the B concentration at the two peaks was decreased and the sheet resistance increased. In contrast, the wafers annealed at 1100°C for between 40 s and 180 s using the SRTF system showed a monotonic decrease of B concentration and a monotonic increase of sheet resistance with annealing time.

To investigate the cause of B concentration fluctuation, SIMS depth profiling of B and F atoms was performed for all wafers annealed using both the lamp-based RTP system and SRTF system. Figure 3 shows B and F depth profiles of wafers annealed for 40 s in the lamp-based RTP system and

wafers annealed for 70 s in the SRTF system at 900°C , 1000°C and 1100°C . Both the B and F depth profiles from the wafers annealed at 900°C and 1000°C in the lamp-based RTP system and SRTF system were almost identical except for those from the wafers annealed at 1100°C . Boron atoms were diffused into the bulk region as the annealing temperature was increased. All of the F profiles were separated into two peaks, regardless of the annealing system. The F atoms did not diffuse into the bulk, but they moved towards the wafer surface as the annealing temperature was increased. Even after the annealing at 1100°C , a large number of F atoms are retained in the implanted region. The influence of the retained F atoms on the electrical property and B diffusion should be investigated in detail. The wafer annealed at 1100°C for 40 s in the lamp-based RTP system showed two B peaks around 65 nm and 105 nm from the surface. The depth of the B peaks corresponded well with that of the F peak positions. The authors speculate that there is a strong correlation between the B and F profiles. The areas of high F concentration seemed to be very efficient in gettering B atoms from neighboring area to form B–F clusters under a very high light illumination environment. The wafer annealed at 1100°C for 70 s in the SRTF system did not show any fluctuation of B concentration with depth.

The annealing time dependency of B and F atoms was investigated at 900°C , 1000°C and 1100°C . Only the wafers annealed at 1100°C for longer than 25 s using the lamp-based RTP system showed fluctuation of B concentration with depth. The B and F depth profiles of wafers annealed at 1100°C using the lamp-based RTP system and SRTF system are plotted in Fig. 4 as a function of annealing time. All of the wafers annealed for 40–110 s using the lamp-based RTP system showed the two B and two F peaks around 65 nm and 105 nm from the wafer surface. The B concentration at the peaks did not change appreciably, while at other depths, the B concentration was reduced significantly by diffusion into the bulk region as the annealing time was increased. The shape of the F profiles did not change significantly, but the concentration of F was reduced even at the two F peaks as the annealing time was increased. In the case of wafers annealed at 1100°C using the SRTF system, no B peak formation was observed even though the F profiles are almost identical with those observed from the wafers annealed using the lamp-based RTP system.

The authors believe that the electrical property of the annealed wafers is strongly correlated with the B and F profiles. At 900°C , the sheet resistance of annealed wafers was monotonically decreased as the annealing time was increased, regardless of the annealing system used, due to a high rate of electrical activation and slow B diffusion. At 1000°C , the sheet resistance of annealed wafers monotonically increased as the annealing time was increased. The decrease of sheet resistance can be explained by the balance between competing processes (i.e., electrical activation and B diffusion). It is likely that if B atoms were almost electrically activated in a very short time due to a very high electrical activation rate at 1000°C , an excessive annealing time would have caused additional B diffusion into the bulk region and resulted in a lower average B concentration. The lower average B concentration results in a higher average resistivity of the implanted region, and consequently a

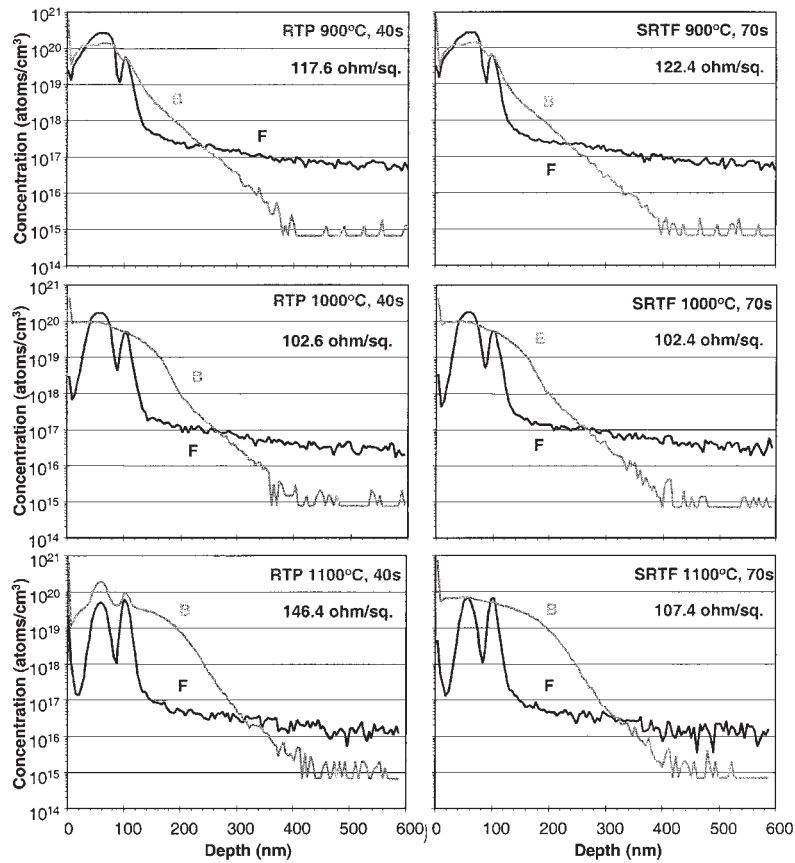


Fig. 3. Annealing temperature dependence of B and F depth profiles of $^{49}\text{BF}_2^+$ ($70\text{ keV } 1 \times 10^{15}\text{ cm}^{-2}$) implanted wafers after annealing.

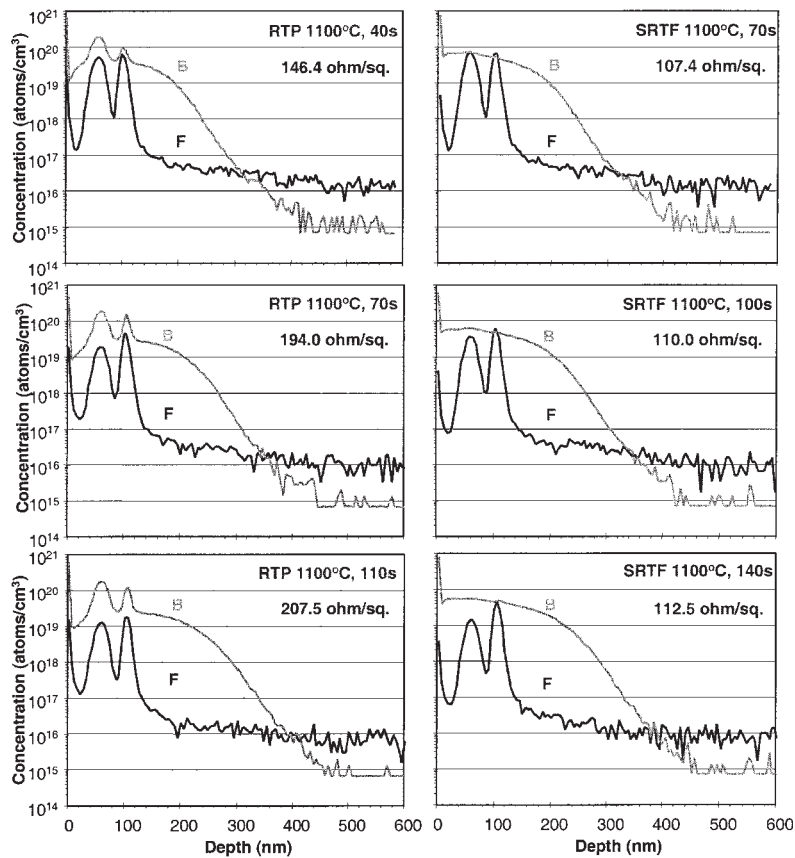


Fig. 4. Annealing time dependence of B and F depth profiles of $^{49}\text{BF}_2^+$ ($70\text{ keV } 1 \times 10^{15}\text{ cm}^{-2}$) implanted wafers after annealing at 1100°C .

higher sheet resistance. At 1100°C, it is much more complex. In the case of wafers annealed using the SRTF system, the sheet resistance of annealed wafers was slowly and monotonically increased as the annealing time was increased. This was very similar to the case of wafers annealed at 1000°C. The same explanation is valid for the sheet resistance increase with increased annealing time. In the case of wafers annealed using the lamp-based RTP system, the sheet resistance of annealed wafers increased at a very high rate as the annealing time was increased. The formation of the B peaks with a very high concentration consumed most of the B atoms in the implanted region. As a result, the number of electrically active B atoms is greatly reduced. This caused the sudden sheet resistance increase in wafers annealed at 1100°C for longer than 25 s using the lamp-based RTP system. As the annealing time increases further, the average B concentration other than the B peaks decreased and resulted in increased sheet resistance. Given that the sheet resistance of wafers annealed using the SRTF system is strongly related to the B depth profiles, the distribution of B atoms in the implanted region dominates the electrical property of the $^{49}\text{BF}_2^+$ implanted region. F atoms are less electrically active but can cause the B peak formation at F peak positions under the high temperature annealing (very strong light illumination) environment of the lamp-based RTP system.

The difference in B depth profiles between wafers annealed using the lamp-based RTP system and those annealed using the SRTF system is caused by the difference in the wafer heating mechanism. The lamp-based RTP system and the SRTF system can be classified as a cold wall system and a hot wall system, respectively. The lamp-based RTP system uses an internal heating mechanism, whereas the SRTF system uses an external heating mechanism. In the lamp-based RTP system, a wafer to be heat-treated absorbs the photon energy emitted by the light source (i.e., tungsten halogen lamps). The wafer temperature is controlled by adjusting the filament temperature (or lamp power). By adjusting the filament temperature, the photon energy distribution from the light source is shifted towards the short wavelength (high photon energy) side at high lamp powers and the long wavelength (lower photon energy) side at low lamp powers. The modulation of lamp power causes the undesirable local and time-dependent fluctuation of photon energy distribution. In contrast, the SRTF system utilizes the combination of conduction, convection and radiation heating mechanisms for wafer heating. Since the furnace (process chamber) temperature is kept constant at the process temperature, the photon energy distribution is also kept constant. The wavelength (photon energy) at the maximum energy density from the furnace (operating at 1100°C) is calculated to be 2.1 μm (0.59 eV) whereas the wavelength (photon energy) for the maximum energy density from the filament heated up to 3000°C is calculated to be 0.9 μm (1.38 eV). The wavelength for the maximum energy density can be calculated by Wien's displacement law ($\lambda m = b/T$, where coefficient $b = 0.002898 \text{ mK}$ and T is temperature in K) for thermal radiation.¹⁰⁾

When the photon energy (wavelength) from the light source matches or exceeds an absorption edge corresponding to those pertaining to the Si–B–F atomic complex and their

compounds, one would expect to see fluctuations of B concentration. This was seen in this study. In the case of maximum (tungsten) filament temperature (around 3000°C), the maximum photon energy emitted through a quartz wall of the (tungsten halogen) lamps is equal to 4.0 eV (300 nm in wavelength). The photon energy of 4.0 eV is sufficiently high to influence Si–B–F atomic complex formation, disassociation and/or redistribution. The B profiles remain about the same over lamp-based RTP annealings of 40, 70 and 110 s at 1100°C while F peaks decrease by a factor of 4. For the SRTF annealing results, the F peaks did not decrease as significantly and no B clustering was observed in wafers annealed for 70, 100 and 140 s at 1100°C.

As annealing time increases, the F concentration in the bulk is significantly decreased and the F concentration at the surface is much higher in wafers annealed by the lamp-based RTA system (Fig. 4). The total amount of F atoms in wafers also decreases with annealing time increase at 1100°C, regardless of the annealing system used. The total F amount in the wafer annealed at 1100°C for 25 s in the lamp-based RTA system is 16% lower than that in the wafer annealed at 1100°C for 55 s in the SRTF system. The total F amount in the wafer annealed at 1100°C for 110 s in the lamp-based RTA system is 38% lower than that in the wafer annealed at 1100°C for 140 s in the SRTF system. All of the lamp-RTA annealed wafers which showed double peaks in B concentration depth profiles showed a significant reduction of F concentration and a significant increase of surface F concentration compared to the SRTF annealed ones.

The authors speculate that the high-energy photon irradiation in the lamp-based RTP system substantially enhances the F redistribution (reduction) as the annealing temperature increases. As the F atoms leave vacancies behind, B starts to cluster near the vacancies (formerly F-rich regions). It is reasonable to believe that high-energy photons are responsible for the fluctuation of B atoms in wafers annealed at 1100°C using the lamp-based RTP system. At a given wafer temperature, the SRTF system always gives a higher surface temperature due to the hot wall-type configuration. Any cold wall-type system which utilizes the internal heating mechanism would cause a maximum temperature below the surface due to radiation heat loss from the surface. The difference in heating mechanism and the cross-sectional temperature profile must be taken into account in analyzing the dopant behavior during annealing in different types of annealing systems. The implant energies and doses must be varied along with annealing methods and conditions to better understand the differences in dopant redistribution and B clustering mechanism between the lamp-based RTP annealing and the resistively heated SRTF annealing.

Optical enhancement effects in diffusion and electrical activation in high-dose (50 keV , $5 \times 10^{15} \text{ cm}^{-2}$) B ion implanted wafers annealed at 800°C have been reported using lamp-based RTP systems, but have not been seen when a single wafer-type vertical furnace is used.¹¹⁾ The enhanced B activation in the lamp-based RTP system was observed under two out of four annealing conditions. The enhancement was explained using the B clustering model proposed by Pelaz *et al.*¹²⁾ However, we did not observe any significant difference in B diffusion or activation between

implanted wafers annealed in the lamp-based RTP system and those annealed in the furnace-based SRTF system in our previous study.⁵⁾ A small difference was observed in the B concentration near the wafer surface. The wafers annealed using the SRTF system showed a higher subsurface B concentration than those annealed using the lamp-based RTP system. The difference is due to the difference in wafer heating mechanism (cold wall vs. hot wall). We have found negative optical effects on diffusion and electrical activation in medium-dose (70 keV , $1 \times 10^{15} \text{ cm}^{-2}$) $^{49}\text{BF}_2^+$ ion implanted wafers annealed at 1100°C for longer than 25 s in the lamp-based RTP system. A continuous study using $^{49}\text{BF}_2^+$ ion implanted wafers with different implant energies and doses is needed to understand the true optical effects on diffusion and electrical activation in implanted wafers during RTA.

$^{49}\text{BF}_2^+$ ion implantation has been widely investigated as an alternative ion species for $^{11}\text{B}^+$ ions in the formation of shallow and ultra-shallow junctions due to their amorphization ability and small projected range compared to $^{11}\text{B}^+$ ions at a given implant energy.^{1,2)} In this study, we have learned that the majority of F atoms implanted as $^{49}\text{BF}_2^+$ ions were retained even after annealing up to 1100°C . A high-temperature annealing helps to reduce the number of F atoms in the implanted region, but it also enhances B diffusion. The high-temperature annealing in the lamp-based RTP system can also cause the B clustering near the F-rich or F-clustered region ($\sim 65 \text{ nm}$ and $\sim 105 \text{ nm}$ depth from the surface) and a large increase in sheet resistance. The annealing process can be optimized for practical usage (a reasonable sheet resistance with a minimal B diffusion). The effects of a high concentration of retained F atoms on device performance and reliability must be investigated. The F atoms can cause degradation of device performance and reliability due to their corrosive characteristics.

4. Summary

RTA of $^{49}\text{BF}_2^+$ (70 keV , $1 \times 10^{15} \text{ cm}^{-2}$) implanted Si wafers (200 mm in diameter) was studied using both a single wafer furnace-type system and a lamp-based system. The sheet resistance and sheet resistance uniformity of the implanted wafers were measured after annealing under various conditions. The B and F depth profiles were measured using SIMS after annealing. It was found that B atoms diffuse into bulk crystal as annealing progresses while

fluorine atoms move towards the surface and form two peculiar peaks around 65 nm and 105 nm from the surface, regardless of annealing conditions. A significant increase in sheet resistance due to boron clustering near the F peaks was observed in wafers annealed at 1100°C using a lamp-based system. B clustering near the F-rich or F-clustered region ($\sim 65 \text{ nm}$ and $\sim 105 \text{ nm}$ from the surface) and a large increase in sheet resistance were observed in wafers annealed at 1100°C using the lamp-based RTP system. The B clustering near the F peaks is explained as an effect of internal heating. The high-energy photons irradiated from the tungsten halogen lamps under a very high-power operation resulted in the enhancement of dopant redistribution and B clustering.

Acknowledgments

The authors would like to thank Mr. K. Kang, Mr. S. Fujimoto, Mr. T. Yamazaki and Mr. J. Schram of Wafer-Masters, Inc. for useful discussions and encouragement throughout this work. The authors also would like to thank Mr. T. Shimotani, Mr. Y. Shirotani and Mr. J. Yamamoto of NEC Hiroshima Limited for the experimental arrangements.

- 1) Y. Kim, H. Z. Massoud and R. B. Fair: *J. Electron. Mater.* **18** (1989) 143.
- 2) M. Uematsu: *Jpn. J. Appl. Phys.* **39** (2000) 1608.
- 3) D. F. Downey, C. M. Osburn and S. D. Markus: *Solid State Technol.* **40-12** (1997) 71.
- 4) J. Park, J. Y. Lee, K. Lee and H. Hwang: *Jpn. J. Appl. Phys.* **37** (1998) L1376.
- 5) W. S. Yoo, T. Fukada, T. Setokubo, K. Aizawa, T. Ohsawa, N. Takahashi and K. Enjoji: *J. Electrochem. Soc.* **149** (2002) G424.
- 6) W. S. Yoo, T. Fukada, H. Kitayama, N. Takahashi, K. Enjoji and K. Sunohara: *Jpn. J. Appl. Phys. Lett.* **39** (2000) L493.
- 7) W. S. Yoo, T. Fukada, H. Kuribayashi, H. Kitayama, N. Takahashi, K. Enjoji and K. Sunohara: *Jpn. J. Appl. Phys. Lett.* **39** (2000) L694.
- 8) W. S. Yoo, T. Fukada, H. Kuribayashi, H. Kitayama, N. Takahashi, K. Enjoji and K. Sunohara: *Jpn. J. Appl. Phys.* **39** (2000) 6143.
- 9) D. Jennings, G. de Cock and M. A. Foad: *Proc. 6th Int. Conf. Advanced Thermal Processing of Semiconductors—RTP'98* (Kyoto), 1998, p. 187.
- 10) F. P. Incropera and D. P. DeWitt: *Fundamentals of Heat and Mass Transfer* (John Wiley & Sons, New York, 1996) Chap. 12.
- 11) R. B. Fair: *Electrochem. Soc. Proc.* **2000-9** (2000) 21.
- 12) L. Pelaz, M. Jaraiz, G. H. Gilmer, H. J. Grossmann, C. S. Rafferty, D. J. Eagleham and J. M. Poate: *Appl. Phys. Lett.* **70** (1997) 2285.